BAREKENG: Journal of Mathematics and Its Applications
September 2025 Volume 19 Issue 3 Page 1649-1666
P-ISSN: 1978-7227 E-ISSN: 2615-3017
https://doi.org/10.30598/barekengvol19iss3pp1649-1666

MATHEMATICAL MODEL OF DENGUE HEMORRHAGIC FEVER SPREAD WITH DIFFERENT LEVELS OF TRANSMISSION RISK

Faishal Farrel Herdicho[1], Nabil Azizul Hakim[2], Fatmawati[3*], Cicik Alfiniyah[4], John Olajide Akanni[5,6]

[1,2,3,4]*Department of Mathematics, Faculty of Science and Technology, Universitas Airlangga*
Jln. Dr. Ir. H. Soekarno, Mulyorejo, Surabaya, 60115, Indonesia

[5]*Department of Mathematics, Saveetha Institute of Medical and Technical Sciences, Saveetha University*
Kachipuram – Chennai Rd, Chennai, Tamil Nadu, 602105, India

[6]*Department of Mathematical and Computing Sciences, Faculty of Applied Sciences, Koladaisi University*
KM 18, Ibadan-Oyo Express Road, Ibadan, Oyo State, 200138, Nigeria

*Corresponding author's e-mail: * **fatmawati@fst.unair.ac.id***

Article History:

Received: 28th December 2024
Revised: 4th February 2025
Accepted: 11th March 2025
Published: 1st July 2025

Keywords:

Dengue Hemorrhagic Fever;
Genetic Algorithm;
Mathematical Model;
Parameter Estimation;
Transmission Risk.

ABSTRACT

Dengue Haemorrhagic Fever (DHF) is a vector-borne disease caused by the dengue virus, transmitted to humans through the bite of an infected female Aedes aegypti mosquito. DHF is prevalent in tropical regions, necessitating mathematical modeling to better understand its dynamics and predict its spread. This study develops and analyzes a mathematical model for DHF transmission that incorporates seven compartments to reflect different transmission risk levels. Stability analysis of the disease-free and endemic equilibria was conducted, with the basic reproduction number (R_0) *used to classify the conditions under which DHF transmission is controlled* $(R_0 < 1)$ *or endemic* $(R_0 > 1)$*. Key model parameters were estimated using DHF case data from East Java in 2018, employing a genetic algorithm (GA) to optimize the estimation process. The GA approach achieved a mean absolute percentage error (MAPE) of* 2.6382%*, ensuring high accuracy in parameter values. Furthermore, the basic reproduction number was determined to be* $R_0 = 1.14$*, which is greater than one, confirming that DHF remains endemic in East Java. Sensitivity analysis identified the mosquito biting rate* (b)*, mosquito mortality rate* (μ_v)*, and transmission rates* $(\beta_h \text{ and } \beta_v)$ *as the most critical factors influencing* R_0*. Numerical simulations demonstrated the effects of these key parameters on both* R_0 *and the symptomatic human population* (I_h)*. An increase in* b*,* β_h*, or* β_v *significantly amplified* R_0 *and* I_h*, while a rise in* μ_v *had the opposite effect, reducing both transmission and infections. These results underscore the critical role of vector control strategies, such as increasing mosquito mortality and reducing breeding sites, in mitigating DHF outbreaks. This study highlights the utility of combining mathematical modeling with genetic algorithm-based parameter estimation to provide accurate insights into disease dynamics and inform effective control measures.*

How to cite this article:

F. F. Herdicho, N. A. Hakim, Fatmawati, C. Alfiniyah, and J. O. Akanni, "MATHEMATICAL MODEL OF DENGUE HEMORRHAGIC FEVER SPREAD WITH DIFFERENT LEVELS OF TRANSMISSION RISK UNDER REAL DATA AND GENETIC ALGORITHM OPTIMIZATION," *BAREKENG: J. Math. & App.*, vol. 19, no. 3, pp. 1649-1666, September, 2025.

Journal homepage: *https://ojs3.unpatti.ac.id/index.php/barekeng/*
Journal e-mail: *barekeng.math@yahoo.com; barekeng.journal@mail.unpatti.ac.id*

Research Article · Open Access

1. INTRODUCTION

Dengue Hemorrhagic Fever (DHF) is a significant public health threat that predominantly impacts tropical and subtropical regions, including Southeast Asia, Latin America, and Africa. This mosquito-borne disease is caused by the dengue virus, a member of the Flavivirus genus within the Flaviviridae family, and is transmitted primarily through the bite of infected female Aedes aegypti mosquitoes [1]. First identified in Manila, Philippines, during 1953 – 1954, DHF quickly established itself as a critical health issue across Southeast Asia within just two decades, becoming a leading cause of pediatric mortality by the mid-1970s [2]. The disease presents a wide clinical spectrum, with approximately 80% of infected individuals experiencing mild fever-like symptoms, typically appearing between 3 to 14 days post-infection [3].

Compared to other diseases and their impacts, DHF puts a huge burden on the human population, the health sector, and the economy in the majority of tropical countries in the world. The emergence and spread of the dengue virus can also pose a global pandemic threat. It is proven that in the last five decades, DHF cases have increased by 30 times. DHF is also the most important arbovirus disease in the world. Every year, DHF infection continues to increase, resulting in hundreds of thousands of people being infected, with medical costs of up to 514-1394 USD per year [4]. In Indonesia, DHF is one of the infectious diseases that is still a major problem for public health, with a very rapid spread and has the potential to cause death. DHF was first reported to occur in 1968 in the city of Surabaya with 58 sufferers and 24 deaths, then spread throughout Indonesia and attacked all ages, especially children [5]. In 2017, the number of dengue cases in East Java reached 7,254 people throughout East Java, with the number of deaths reaching 104 residents [6].

Understanding and predicting DHF transmission dynamics are essential for formulating effective intervention strategies. Over the past two decades, mathematical modeling has emerged as a powerful tool for studying the spread of infectious diseases, including DHF [7], [8], [9], [10]. Previous studies have provided significant insights into various aspects of dengue epidemiology. For instance, Agusto and Khan [11] integrated vaccination strategies into their model, while Jan et al. [12] explored the role of asymptomatic infections in disease dynamics. Ghosh et al. [13] introduced a model that distinguishes between high-risk and low-risk susceptible populations, and Anggriani et al. [14] focused on reinfection with the same serotype. More recently, Zhang et al. [15] proposed innovative control mechanisms involving Wolbachia bacteria to disrupt mosquito reproduction. Most existing mathematical models either rely on static parameters derived from limited datasets or lack specificity to regional epidemiological contexts. Furthermore, while parameter estimation is critical for translating theoretical models into practical applications, challenges persist in accurately calibrating models to real-world data.

Genetic algorithm (GA) is a population-based optimization method inspired by natural selection mechanisms such as selection, mutation, and recombination to find the best solution to a given problem [16]. Compared to conventional parameter estimation methods, GA offers several key advantages. GA does not require function derivatives or specific assumptions about data distribution, making it more flexible for solving complex and nonlinear optimization problems. Additionally, GA can explore a wide range of possible solutions, reducing the risk of getting stuck in suboptimal solutions. This capability makes GA particularly effective in determining the best parameters for epidemiological models with multiple variables and uncertainties. Therefore, in this study, GA is utilized to estimate model parameters, ensuring that simulation results closely align with real-world data.

Despite the numerous mathematical models developed for DHF, existing models often have limitations in capturing the heterogeneity in transmission risk and in accurately estimating parameters from real-world data. Many models assume uniform transmission dynamics, which may not reflect the actual variations in risk levels among infected individuals. Moreover, traditional parameter estimation methods may not provide the best fit for epidemiological trends. These gaps highlight the need for a refined mathematical model that incorporates different levels of transmission risk and employs a robust estimation technique to improve predictive accuracy. This study seeks to address these issues by developing an extended DHF model with a compartment for transmission risk levels and utilizing a genetic algorithm to optimize parameter estimation.

In this study, we aim to address modifying and extending the DHF models proposed by Jan et al. [12] and Ghosh et al. [13]. Utilizing monthly cumulative DHF case data from East Java in 2018, we apply genetic algorithms to estimate parameters within the models. This approach not only enhances the realism and predictive accuracy of the models but also provides novel insights into the dynamics of DHF transmission. By integrating regional data and advanced parameter estimation techniques, this research seeks to offer a more targeted and effective framework for DHF control. The findings are expected to inform public health

strategies and contribute to reducing the morbidity and mortality associated with DHF in East Java and similar endemic regions in the future.

2. RESEARCH METHODS

In this section, we provide a detailed explanation of the model formulation and the step-by-step implementation of the Genetic Algorithm (GA) as an optimization technique.

2.1 DHF Model Formulation

This study builds upon and modifies the mathematical models for dengue haemorrhagic fever (DHF) transmission previously developed by Jan et al. [12] and Ghosh et al. [13]. The resulting model incorporates the dynamics of DHF transmission with varying levels of risk, reflecting environmental and population-specific factors. In this model, we assume a constant total population size. This assumption aligns with previous studies that serve as our primary references [12]. While real-world populations are dynamic, the relatively short time frame of this study minimizes the impact of demographic changes on disease transmission dynamics. Other assumptions in the model include:

1. The susceptible human population is divided into two compartments, S_h and L_h, which differ based on environmental risk factors.
2. The infected human population is divided into two compartments, A_h (asymptomatic infections) and I_h (symptomatic infections), both of which can transition to the recovered compartment (R_h).
3. Humans who recover from dengue are assumed to gain permanent immunity, as the likelihood of reinfection with the same serotype is negligible.
4. Mortality due to DHF is not considered in this model.
5. I_h population can recover either naturally or through treatment.
6. The incubation period for the dengue virus is assumed to be negligible, allowing infected individuals to transmit the virus immediately upon infection.
7. Age and sex differences within the human population are not accounted for in the model.

The notations and descriptions for each compartment and parameter used in the model are summarized in Table 1 and Table 2. These tables provide clarity regarding the biological meaning of the variables and parameters, ensuring accurate interpretation of the model.

Table 1. Compartments Description

Compartments	Description
S_h	Number of high-risk susceptible human population
L_h	Number of low-risk susceptible human population
A_h	Number of asymptomatic human population
I_h	Number of symptomatic human population
R_h	Number of recovered human population
S_v	Number of susceptible mosquito population
I_v	Number of infected mosquito population

Table 2. Parameters Description

Parameters	Description	Unit
r	Proportion of newly recruited individuals joining the high-risk susceptible class	-
Ψ	Proportion of asymptomatic carriers	-

Parameters	Description	Unit
γ	Recovery rate of human individuals	Month^{-1}
τ	Treatment rate, which I_h recover	Month^{-1}
b	Biting rate of mosquitoes	Month^{-1}
μ_h	Natural mortality rate of humans	Month^{-1}
μ_v	Natural mortality rate of mosquitoes	Month^{-1}
β_h	Transmission probability from infected mosquitoes to susceptible humans	-
β_v	Transmission probability from infected humans to susceptible mosquitoes	-

Table 1 describes the compartments that represent different groups within the human and mosquito populations. The human population is divided into several categories: high-risk and low-risk susceptible individuals (S_h and L_h), asymptomatic carriers (A_h), symptomatic infected individuals (I_h), and those who have recovered from the disease (R_h). These divisions capture variations in risk level, infection status, and immunity. Meanwhile, the mosquito population is categorized into susceptible (S_v) and infected (I_v) groups, reflecting their role in disease transmission.

Table 2 outlines the parameters that influence the dynamics of the model. These parameters include proportions, such as the fraction of newly recruited humans joining the high-risk group (r) and the proportion of asymptomatic carriers among infected humans(Ψ). Rates such as recovery (γ) and treatment (τ) are included to capture the progression of the disease and the impact of interventions. Transmission rates (β_h and β_v) describe how the disease spreads between humans and mosquitoes, while the biting rate (b) captures mosquito feeding behavior. Additionally, natural mortality rates of humans (μ_h) and mosquitoes (μ_v) are incorporated to account for baseline population turnover.

Based on these assumptions, the description of compartments and parameters, the transmission dynamics of the DHF model are illustrated in the diagram presented in **Figure 1**. This diagram serves as a conceptual representation of the interactions and transitions among the various compartments in the system.

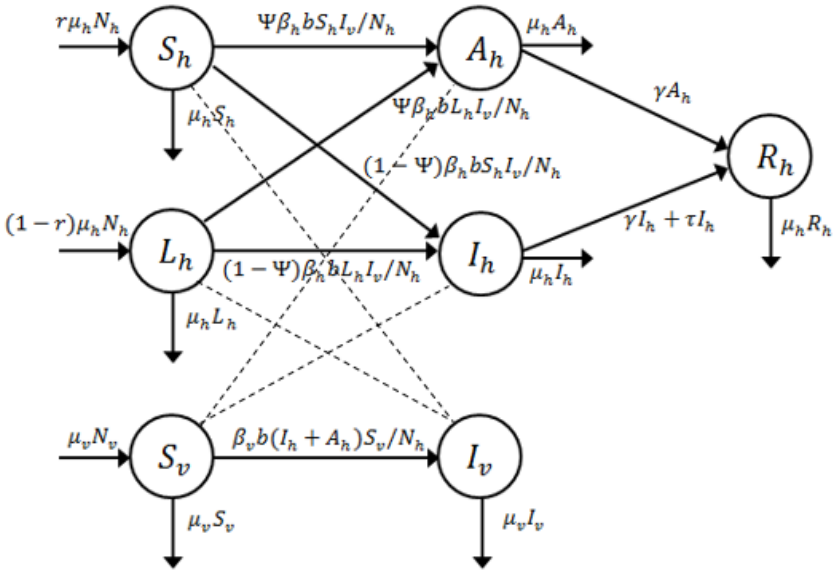

Figure 1. DHF Transmission Diagram

Based on the transmission diagram presented above, the system of differential equations for the mathematical model of DHF spread is formulated as follows:

$$\frac{dS_h}{dt} = r\mu_h N_h - b\frac{\beta_h S_h I_v}{N_h} - \mu_h S_h,$$
$$\frac{dL_h}{dt} = (1-r)\mu_h N_h - b\frac{\beta_h L_h I_v}{N_h} - \mu_h L_h,$$

$$\begin{aligned}
\frac{dA_h}{dt} &= \Psi b\frac{\beta_h(S_h+L_h)I_v}{N_h} - (\mu_h+\gamma)A_h,\\
\frac{dI_h}{dt} &= (1-\Psi)b\frac{\beta_h(S_h+L_h)I_v}{N_h} - (\mu_h+\gamma+\tau)I_h,\\
\frac{dR_h}{dt} &= \gamma(A_h+I_h)+\tau I_h - \mu_h R_h,\\
\frac{dS_v}{dt} &= \mu_v N_v - b\frac{\beta_v S_v(A_h+I_h)}{N_h} - \mu_v S_v,\\
\frac{dI_v}{dt} &= b\frac{\beta_v S_v(A_h+I_h)}{N_h} - \mu_v I_v.
\end{aligned} \tag{1}$$

The variables S_h, L_h, A_h, I_h, R_h, S_v and I_v are all non-negative. The total human population is given by $N_h = S_h + L_h + A_h + I_h + R_h \geq 0$ and the total mosquito population is $N_v = S_v + I_v \geq 0$. Additionally, all parameters defined in the model are positive, with $0 \leq r, \Psi \leq 1$ as proportion or probabilities and $\gamma, \tau, b, \mu_h, \mu_v, \beta_h, \beta_v > 0$.

2.2 Genetic Algorithm

The application of Genetic Algorithm (GA) in this study follows a systematic approach designed to optimize the parameters of the model. GA is a population-based optimization method inspired by natural selection mechanisms such as selection, mutation, and recombination to find the best solution to a given problem. GA does not require function derivatives or specific assumptions about data distribution, making it more flexible for solving complex and nonlinear optimization problems. Additionally, GA can explore a wide range of possible solutions, reducing the risk of getting stuck in suboptimal solutions **[16]**. The key steps in the GA process are as follows:

1. Initialization: The first step involves defining the problem parameters, including the number of variables, population size, mutation rate, crossover rate, and the number of generations. The algorithm also specifies the upper and lower bounds for the model parameters. A random initial population is generated, with each solution corresponding to a set of model parameters within the defined bounds.
2. Evaluation: Each individual in the population is evaluated by solving the system numerically with its parameters. The model's predictions are compared to actual data, and the error of Mean Absolute Percentage Error (MAPE) is calculated to assess the fit of each solution.
3. Selection: Individuals are ranked based on their error values (MAPE). The top-ranked individuals are selected as parents for the next generation, with a number proportional to the crossover rate.
4. Crossover: The selected parents undergo crossover, where their model parameters are combined to produce offspring, exchanging genetic information to potentially improve the solutions.
5. Mutation: To maintain genetic diversity, a mutation process is applied, where a percentage of the offspring have their parameters randomly altered within the defined bounds.
6. Replacement: The offspring replace the least fit individuals in the population, forming a new generation.
7. Iteration: Steps 2 – 6 are repeated for a set number of generations. Over time, the population evolves toward better solutions, with the best set of parameters found in the final generation being selected as the optimal model parameters.

2.3 Research Methodology

This study employs a mathematical modeling approach to analyze the transmission dynamics of Dengue Hemorrhagic Fever (DHF). The research methodology in **Figure 2** consists of several key stages, including model formulation, parameter estimation, stability analysis, and numerical simulation.

1. Model Formulation

   The mathematical model is constructed based on a compartmental framework, incorporating different population groups to represent disease transmission dynamics. The model extends previous studies by integrating varying levels of transmission risk and employing a system of differential equations to describe interactions between humans and mosquito populations.

2. Parameter Estimation

   The model parameters are estimated using actual DHF case data from East Java Province in 2018. Since some parameters related to mosquito populations are not directly available from official records, a genetic algorithm (GA) is employed to optimize parameter values and minimize discrepancies between simulated and observed data.

3. Stability Analysis

   The stability of the model is examined through equilibrium analysis, focusing on disease-free and endemic conditions. The basic reproduction number (R_0) is derived to determine the threshold conditions under which DHF can either persist or be eradicated. Sensitivity analysis is also conducted to identify the most influential parameters affecting R_0.

4. Numerical Simulation

   To observe long-term trends in DHF transmission, numerical simulations are performed using estimated parameter values. Two scenarios are considered: (i) a disease-free scenario with $R_0 < 1$, where infection gradually disappears, and (ii) an endemic scenario with $R_0 > 1$, where the disease continues to spread.

The overall research methodology is illustrated in the following flowchart:

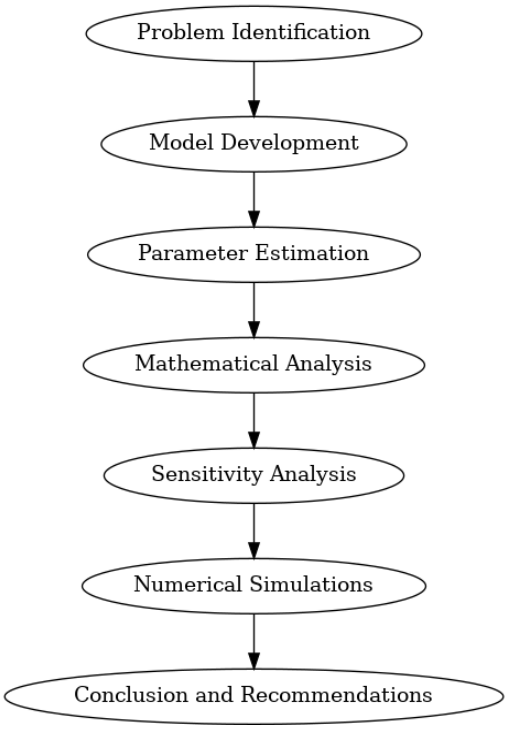

Figure 2. Flowchart of Research

3. RESULTS AND DISCUSSION

3.1 Positive Invariance and Boundedness

To show the boundedness of the solution, we consider the total human and mosquito populations. From system **Equation (1)**, the total human population satisfies:

$$\frac{dN_h}{dt} = \frac{dS_h}{dt} + \frac{dL_h}{dt} + \frac{dA_h}{dt} + \frac{dI_h}{dt} + \frac{dR_h}{dt}$$
$$\frac{dN_h}{dt} = \mu_h N_h - \mu_h(S_h + L_h + A_h + I_h + R_h)$$
$$\frac{dN_h}{dt} = \mu_h N_h - \mu_h N_h$$
$$\frac{dN_h}{dt} = 0$$

Thus, the total human population remains $N_h = K_1$, where $K_1 = S_h(0) + L_h(0) + A_h(0) + I_h(0) + R_h(0)$. Similarly, for the mosquito population, using the same approach, we obtain that the total mosquito population remains $N_v = K_2$, where $K_2 = S_v(0) + L_v(0)$. Therefore, the solutions of system **Equation (1)** remain non-negative for all time $t > 0$ and defined in the closed set Ω (positively invariant) given as

$$\Omega = \Omega_h \cup \Omega_v \subset \mathbb{R}_+^5 \times \mathbb{R}_+^2,$$

where

$$\Omega_h = \left\{\left(S_h(t), L_h(t), A_h(t), I_h(t), R_h(t)\right) \in \mathbb{R}_+^5 : N_h = K_1 = S_h(0) + L_h(0) + A_h(0) + I_h(0) + R_h(0)\right\},$$
$$\Omega_v = \left\{\left(S_v(t), I_v(t)\right) \in \mathbb{R}_+^2 : N_v = K_2 = S_v(0) + I_v(0)\right\},$$

with K_1 and K_2 are constant values.

Next, we show the positivity solution of system **Equation (1)** based on the following theorem.

Theorem 1. *Let $S_h(0)$, $L_h(0)$, $A_h(0)$, $I_h(0)$, $R_h(0)$, $S_v(0)$ and $I_v(0)$ be the initial conditions of the system. If $S_h(0) \geq 0$, $L_h(0) \geq 0$, $A_h(0) \geq 0$, $I_h(0) \geq 0$, $R_h(0) \geq 0$, $S_v(0) \geq 0$ and $I_v(0) \geq 0$ then all solutions are positive for every $t \geq 0$.*

Proof. Take the first equation in the system **Equation (1)**, and assume that $\lambda(t) = b\frac{\beta_h I_v(t)}{N_h}$ as follows

$$\frac{dS_h}{dt} = r\mu_h N_h - \lambda(t)S_h(t) - \mu_h S_h(t)$$
$$\frac{dS_h}{dt} \geq -\lambda(t)S_h(t) - \mu_h S_h(t)$$
$$\frac{d\left(e^{\mu_h t + \int_0^t \lambda(s)ds} S_h(t)\right)}{dt} \geq 0$$
$$S_h(t) \geq ke^{-\mu_h t - \int_0^t \lambda(s)ds}$$

with the initial condition $S_h(0)$ at $t = 0$, we get

$$S_h(t) \geq S_h(0)e^{-\mu_h t - \int_0^t \lambda(s)ds}.$$

Hence $S_h(t)$ is positive for $t \geq 0$ if $S_h(0) \geq 0$. Then, using the same steps, we can prove that all compartments are also positive for $t \geq 0$ if the initial conditions of the system are positive.

■

3.2 Parameter Estimation

To optimize the estimation of model parameters, a genetic algorithm (GA) is implemented. GA is an evolutionary optimization technique inspired by natural selection, making it particularly effective for solving

complex, non-linear problems. First, the data used for parameter estimation consists of monthly cumulative DHF case data from January 2018 to December 2018 in East Java Province, obtained directly from the Surabaya Health Office. The value of μ_h is the inverse of the life expectancy in East Java, which is 70.97 years or 70.97×12 months. Thus $\mu_h = \frac{1}{70.97 \times 12}$. The total population of East Java in 2018 is recorded as 39,500,900 individuals [17], [18]. The parameter estimation process involves 14 variables, referred to as "genes" in the context of the genetic algorithm. These genes include remaining parameters, as well as the initial population sizes for compartments where direct data is unavailable. The first to 14th genes are τ, γ, r, Ψ, b, β_h, β_v, μ_v, $S_h(0)$, $L_h(0)$, $A_h(0)$, $R_h(0)$, $S_v(0)$, and $I_v(0)$, respectively.

Table 3. Best Result of Parameter Estimation

Notation	Value	Notation	Value
τ	0.5430	$S_h(0)$	20,043,511
γ	0.5999	$L_h(0)$	19,454,975
r	0.0043	$A_h(0)$	368
Ψ	0.5622	$R_h(0)$	940
b	0.5891	$S_v(0)$	43,016,346
β_h	0.7194	$I_v(0)$	4,006
β_v	0.4986		
μ_v	0.1350		

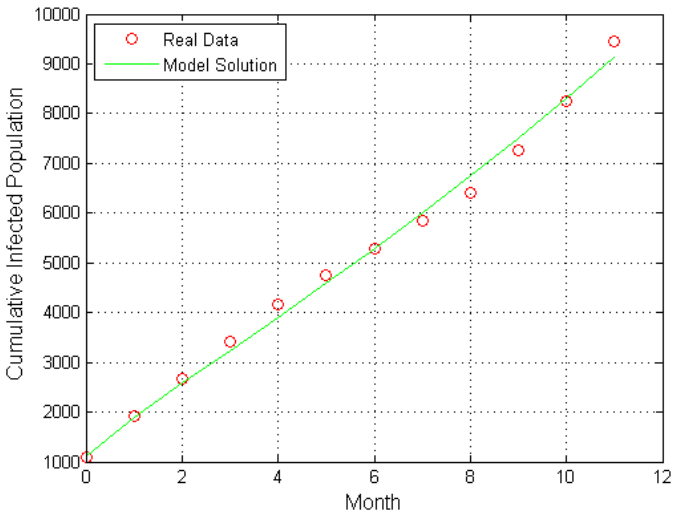

Figure 3. Comparison of Real Data and Model Solution based on Parameter Estimation Results

The estimated parameter values of the DHF model **Equation (1)** are listed in **Table 3**. Based on the parameter values of **Table 3**, the value of R_0 is 1.14. **Figure 3** shows a comparison between the DHF case real data and the model's predictions using the estimated parameters. The results demonstrate a high degree of alignment, with an error difference of only 3.00%. This indicates that the genetic algorithm successfully captured the dynamics of DHF transmission in East Java during the study period. From the graph, it is evident that both the observed data and the model predictions exhibit an increasing trend in DHF cases, although slight discrepancies occur in certain months. The estimated parameters reveal that the transmission rate of the dengue virus from mosquitoes to humans is relatively high, while the transmission rate from humans to mosquitoes is comparatively lower. This asymmetry can be attributed to factors such as population growth, challenges in vector control, and unpredictable climatic and environmental changes. Additionally, the recovery rate for humans, whether through natural or treatment recovery, is found to be substantial. This is consistent with advancements in DHF research, which have significantly improved recovery outcomes in recent years.

3.3 Stability Analysis of Equilibrium Point

This section analyzes the equilibria of system **Equation (1)**. Notice that the total human and mosquito populations are constant, satisfying $\frac{dN_h}{dt} = 0$ and $\frac{dN_v}{dt} = 0$. Consequently, two types of equilibria are identified: the disease-free equilibrium and the endemic equilibrium.

The disease-free equilibrium represents a condition where no dengue virus is present in either the human or mosquito populations. This occurs when there are no infected humans or mosquitoes $(A_h = I_h = I_v = 0)$, and consequently, there are no humans recovering or undergoing treatment $(R_h = 0)$. The disease-free equilibrium is given by:

$$E^0 = \left(S_h^0, L_h^0, A_h^0, I_h^0, R_h^0, S_v^0, I_v^0\right) = (rN_h, (1-r)N_h, 0,0,0, N_v, 0).$$

Next, the basic reproduction number (R_0) is determined, which is used to measure the potential spread of DHF in a population. With the Next Generation Matrix (NGM) method **[19]**. First, we define F as the transmission matrix, whose elements represent the number of newly infected individuals resulting from interactions with the A_h, I_h, and I_v compartments. Meanwhile, Z is the transition matrix, which contains the infected population dynamics without including transmission interaction.

In calculating R_0, we consider only the equations related to the A_h, I_h, and I_v compartments. Based on this approach, the matrices F and Z are derived as follows:

$$F = \begin{pmatrix} \Psi b \frac{\beta_h (S_h + L_h) I_v}{N_h} \\ (1-\Psi) b \frac{\beta_h (S_h + L_h) I_v}{N_h} \\ b \frac{\beta_v S_v (A_h + I_h)}{N_h} \end{pmatrix} \text{ and } Z = \begin{pmatrix} (\mu_h + \gamma) A_h \\ (\mu_h + \gamma + \tau) I_h \\ \mu_v I_v \end{pmatrix}.$$

Let $\mathbb{F}$ and $\mathbb{Z}$ be the Jacobian matrices of the transmission matrix F and the transition matrix Z, evaluated at the disease-free equilibrium (E^0), we obtain:

$$\mathbb{F} = \begin{pmatrix} 0 & 0 & \Psi \beta_h b \\ 0 & 0 & (1-\Psi)\beta_h b \\ \frac{\beta_v b N_v}{N_h} & \frac{\beta_v b N_v}{N_h} & 0 \end{pmatrix} \text{ and } \mathbb{Z} = \begin{pmatrix} \mu_h + \gamma & 0 & 0 \\ 0 & \mu_h + \gamma + \tau & 0 \\ 0 & 0 & \mu_v \end{pmatrix}.$$

The basic reproduction number R_0 is determined as the largest eigenvalue (spectral radius) of the matrix $\mathbb{F}\mathbb{Z}^{-1}$. Thus, we obtain:

$$R_0 = \sqrt{\frac{(\Psi\tau + \gamma + \mu_h)\beta_h \beta_v b^2 N_v}{(\gamma + \mu_h)(\tau + \gamma + \mu_h)\mu_v N_h}},$$

Based on the parameters estimation result in **Table 3**, R_0 is calculated to be 1.14, indicating that $R_0 > 1$ and validating the existence of endemic conditions in East Java Province in 2018.

The endemic equilibrium describes a state where DHF is actively transmitted, resulting in infected humans and mosquitoes $(A_h, I_h, I_v \neq 0)$. The endemic equilibrium, denoted as $E^* = (S_h^*, L_h^*, A_h^*, I_h^*, R_h^*, S_v^*, I_v^*)$, is expressed as:

$$\begin{aligned} S_h^* &= r \frac{\mu_h N_h^2}{\beta_h b I_v^* + \mu_h N_h}, \\ L_h^* &= (1-r) \frac{\mu_h N_h^2}{\beta_h b I_v^* + \mu_h N_h}, \\ A_h^* &= \Psi \frac{\beta_h b (S_h^* + L_h^*) I_v^*}{(\mu_h + \gamma) N_h}, \\ I_h^* &= (1-\Psi) \frac{\beta_h b (S_h^* + L_h^*) I_v^*}{(\mu_h + \gamma + \tau) N_h}, \\ R_h^* &= \frac{\gamma (A_h^* + I_h^*) + \tau I_h^*}{\mu_h}, \end{aligned}$$

$$S_v^* = \frac{\mu_v N_v N_h}{\beta_v b(A_h^* + I_h^*) + \mu_v N_h},$$
$$I_v^* = \frac{(R_0^2 - 1)(\mu_h + \gamma)(\mu_h + \gamma + \tau)\mu_h \mu_v N_h}{(\mu_h + \gamma + \Psi\tau)\beta_h \beta_v b^2 \mu_h + (\mu_h + \gamma)(\mu_h + \gamma + \tau)\mu_v b \beta_h},$$

This equilibrium exists if $R_0^2 > 1 \Leftrightarrow R_0 > 1$.

3.3.1 Local Stability of the Disease-free Equilibrium

The stability of the disease-free equilibrium point is obtained by substituting the value of the disease-free equilibrium (E^0) into the Jacobian matrix as follows:

$$J(E^0) = \begin{pmatrix} -\mu_h & 0 & 0 & 0 & 0 & 0 & -r\beta_h b \\ 0 & -\mu_h & 0 & 0 & 0 & 0 & -(1-r)\beta_h b \\ 0 & 0 & -(\gamma + \mu_h) & 0 & 0 & 0 & \Psi\beta_h b \\ 0 & 0 & 0 & -(\tau + \gamma + \mu_h) & 0 & 0 & (1-\Psi)\beta_h b \\ 0 & 0 & \gamma & \tau + \gamma & -\mu_h & 0 & 0 \\ 0 & 0 & -\frac{\beta_v b N_v}{N_h} & -\frac{\beta_v b N_v}{N_h} & 0 & -\mu_v & 0 \\ 0 & 0 & \frac{\beta_v b N_v}{N_h} & \frac{\beta_v b N_v}{N_h} & 0 & 0 & -\mu_v \end{pmatrix}.$$

From the matrix $J(E^0)$, we will look for the characteristic equation with $|\lambda I - J(E^0)|$, such that we obtain:

$$(\lambda + \mu_h)^3(\lambda + \mu_v)(\lambda^3 + a_1\lambda^2 + a_2\lambda + a_3) = 0, \quad (2)$$

where

$$a_1 = (\gamma + \mu_h) + (\tau + \gamma + \mu_h) + \mu_v,$$
$$a_2 = (\gamma + \mu_h)(\tau + \gamma + \mu_h) + (\gamma + \mu_h)\mu_v + (\tau + \gamma + \mu_h)\mu_v[1 - R_1],$$
$$a_3 = (\gamma + \mu_h)(\tau + \gamma + \mu_h)\mu_v[1 - R_0^2],$$

with $R_1 = \frac{\beta_h \beta_v b^2 N_v}{(\tau+\gamma+\mu_h)\mu_v N_h}$.

From **Equation (2)**, we have the eigenvalues $\lambda_1 = \lambda_2 = \lambda_3 = -\mu_h$, $\lambda_4 = -\mu_v$, which are negative, and the remainder are the roots of the following equation:

$$\lambda^3 + a_1\lambda^2 + a_2\lambda + a_3 = 0. \quad (3)$$

By using the Routh-Hurwitz criterion, the characteristic **Equation (3)** will have roots with negative real parts if and only if $a_1, a_2, a_3, a_1a_2 - a_3 > 0$. It is clear that the coefficient $a_1 > 0$, while $a_2 > 0$ if $R_1 < 1$, and the coefficient $a_3 > 0$ if $R_0^2 < 1$. Using some algebraic calculations, we have

$$a_1a_2 - a_3 = \big((\gamma + \mu_h) + (\tau + \gamma + \mu_h)\big)\big((\gamma + \mu_h)(\tau + \gamma + \mu_h) + (\gamma + \mu_h)\mu_v + (\tau + \gamma + \mu_h)\mu_v[1 - R_1]\big)$$
$$+(\gamma + \mu_h)\mu_v^2 + (\tau + \gamma + \mu_h)\mu_v^2[1 - R_1] + (\gamma + \mu_h)(\tau + \gamma + \mu_h)\mu_v R_0^2.$$

Hence, the coefficient $a_1a_2 - a_3 > 0$ if $R_1 < 1$. Next, we will look for the relationship between R_0^2 and R_1, using some algebraic calculations, we have

$$R_0^2 - R_1 = \frac{(\tau + \gamma + \mu_h)\Psi\beta_h\beta_v b^2 \mu_v N_v N_h}{(\gamma + \mu_h)(\tau + \gamma + \mu_h)^2 \mu_v^2 N_h^2}.$$

Hence, $R_0^2 - R_1 > 0 \Leftrightarrow R_1 < R_0^2$. So, when $R_0^2 < 1$ then $R_1 < 1$ is fulfilled. Then, the conditions are sufficient and necessary for **Equation (2)** to have negative real parts when $R_0^2 < 1 \Leftrightarrow R_0 < 1$. Therefore, the disease-free equilibrium (E^0) will be locally asymptotically stable for $R_0 < 1$ and unstable whenever $R_0 > 1$. The foregoing discussion could be summarized in the following theorem.

Theorem 2. *The disease-free equilibrium* (E^0) *of the system is locally asymptotically stable in the region* Ω *if* $R_0 < 1$ *and unstable if* $R_0 > 1$.

3.3.2 Global Stability of the Disease-free Equilibrium

The global stability of the disease-free equilibrium will be investigated using the direct Lyapunov method. Suppose the positive constants $c_i > 0$, $(i = 1,2,3)$ are defined as:

$$c_1 = \frac{(\mu_h+\gamma+\tau)b\beta_v S_v^0}{N_h},\ c_2 = \frac{(\mu_h+\gamma)b\beta_v S_v^0}{N_h} \text{ and } c_3 = (\mu_h+\gamma)(\mu_h+\gamma+\tau).$$

Then, consider the Lyapunov function $\mathcal{L} : \Omega \to \mathbb{R}$ defined as

$$\mathcal{L} = c_1 A_h + c_2 I_h + c_3 I_v.$$

Time derivative of $\mathcal{L}$ is:

$$\begin{aligned}\frac{d\mathcal{L}}{dt} &= c_1\frac{dA_h}{dt} + c_2\frac{dI_h}{dt} + c_3\frac{dI_v}{dt}\\ &= \left(b\frac{\beta_v S_v}{N_h}c_3 - (\mu_h+\gamma)c_1\right)A_h + \left(b\frac{\beta_v S_v}{N_h}c_3 - (\mu_h+\gamma+\tau)c_2\right)I_h\\ &\quad + \left(\Psi b\frac{\beta_h(S_h+L_h)}{N_h}c_1 + (1-\Psi)b\frac{\beta_h(S_h+L_h)}{N_h}c_2 - \mu_v c_3\right)I_v.\end{aligned}$$

Replacing constant c_1, c_2 and c_3, we obtain:

$$\begin{aligned}\frac{d\mathcal{L}}{dt} &= \frac{b\beta_v(\mu_h+\gamma)(\mu_h+\gamma+\tau)}{N_h}(S_v - S_v^0)A_h + \frac{b\beta_v(\mu_h+\gamma)(\mu_h+\gamma+\tau)}{N_h}(S_v - S_v^0)I_h\\ &\quad + \left(\frac{\Psi b^2\beta_h\beta_v(\mu_h+\gamma+\tau)(S_h+L_h)S_v^0}{N_h^2} + \frac{(1-\Psi)b^2\beta_h\beta_v(\mu_h+\gamma)(S_h+L_h)S_v^0}{N_h^2}\right.\\ &\quad \left. - \mu_v(\mu_h+\gamma)(\mu_h+\gamma+\tau)\right)I_v.\end{aligned}$$

Since $S_v \le S_v + I_v = N_v = S_v^0$, we have $S_v \le S_v^0$, leading to the inequality:

$$\begin{aligned}\frac{d\mathcal{L}}{dt} &\le \left(\frac{\Psi b^2\beta_h\beta_v(\mu_h+\gamma+\tau)(S_h+L_h)S_v^0}{N_h^2} + \frac{(1-\Psi)b^2\beta_h\beta_v(\mu_h+\gamma)(S_h+L_h)S_v^0}{N_h^2} - \mu_v(\mu_h+\gamma)(\mu_h+\gamma+\tau)\right)I_v\\ &\le \mu_v(\mu_h+\gamma)(\mu_h+\gamma+\tau)\left(\frac{\Psi b^2\beta_h\beta_v(S_h+L_h)S_v^0}{N_h^2\mu_v(\mu_h+\gamma)} + \frac{(1-\Psi)b^2\beta_h\beta_v(S_h+L_h)S_v^0}{N_h^2\mu_v(\mu_h+\gamma+\tau)} - 1\right)I_v\\ &\le \mu_v(\mu_h+\gamma)(\mu_h+\gamma+\tau)\left(\frac{(\Psi\tau+\mu_h+\gamma)b^2\beta_h\beta_v(S_h+L_h)S_v^0}{N_h^2\mu_v(\mu_h+\gamma)(\mu_h+\gamma+\tau)} - 1\right)I_v.\end{aligned}$$

Now, using the fact that $S_h + L_h \le S_h + L_h + A_h + I_h + R_h = N_h$, we get $S_h + L_h < N_h$. Also, since $S_v^0 = N_v$, we have:

$$\begin{aligned}\frac{d\mathcal{L}}{dt} &\le \mu_v(\mu_h+\gamma)(\mu_h+\gamma+\tau)\left(\frac{(\Psi\tau+\mu_h+\gamma)b^2\beta_h\beta_v N_h N_v}{N_h^2\mu_v(\mu_h+\gamma)(\mu_h+\gamma+\tau)} - 1\right)I_v\\ &\le \mu_v(\mu_h+\gamma)(\mu_h+\gamma+\tau)(R_0^2 - 1)I_v.\end{aligned}$$

Therefore $\frac{d\mathcal{L}}{dt} \le 0$ if $R_0 \le 1$, with $\frac{d\mathcal{L}}{dt} = 0$ if $R_0 = 1$ or $I_v = 0$. According to LaSalle's invariance principle [20], the free-disease equilibrium (E^0) is globally asymptotically stable in the region Ω if $R_0 < 1$. The foregoing discussion could be summarized in the following theorem.

Theorem 3. *The disease-free equilibrium* (E^0) *of the system is globally asymptotically stable in the region* Ω *if* $R_0 < 1$.

3.3.3 Stability of the Endemic Equilibrium

Due to the analytical complexity of determining the stability of the endemic equilibrium, we investigate its stability through numerical methods. In this simulation, we employ three different initial conditions while keeping the parameter values constant to observe the convergence of the trajectories over an extended period. The initial values used in the numerical simulation are provided in **Table 4**, while the parameter values are based on the estimation results in **Table 3**, except for $N_h = 40{,}000{,}000$ and $N_v = 43{,}000{,}000$.

Table 4. Initial Value for Phase Field Simulation

Initial Value	$S_h(0)$	$L_h(0)$	$A_h(0)$	$I_h(0)$	$R_h(0)$	$S_v(0)$	$I_v(0)$	Color
z_1	20,000,000	19,900,000	30,000	40,000	30,000	42,900,000	100,000	Red
z_2	18,000,000	21,900,000	10,000	50,000	40,000	42,800,000	200,000	Green
z_3	22,000,000	17,900,000	20,000	80,000	20,000	42,600,000	400,000	Blue

For the phase-space simulation, we present a 3D visualization focusing on the A_h, I_h and I_v populations. This approach highlights the equilibrium state for endemic conditions, where the populations are non-zero, and for disease-free conditions, where they are zero. This distinction offers a clear visual representation of the two scenarios. The results of the simulation are illustrated in **Figure 4**.

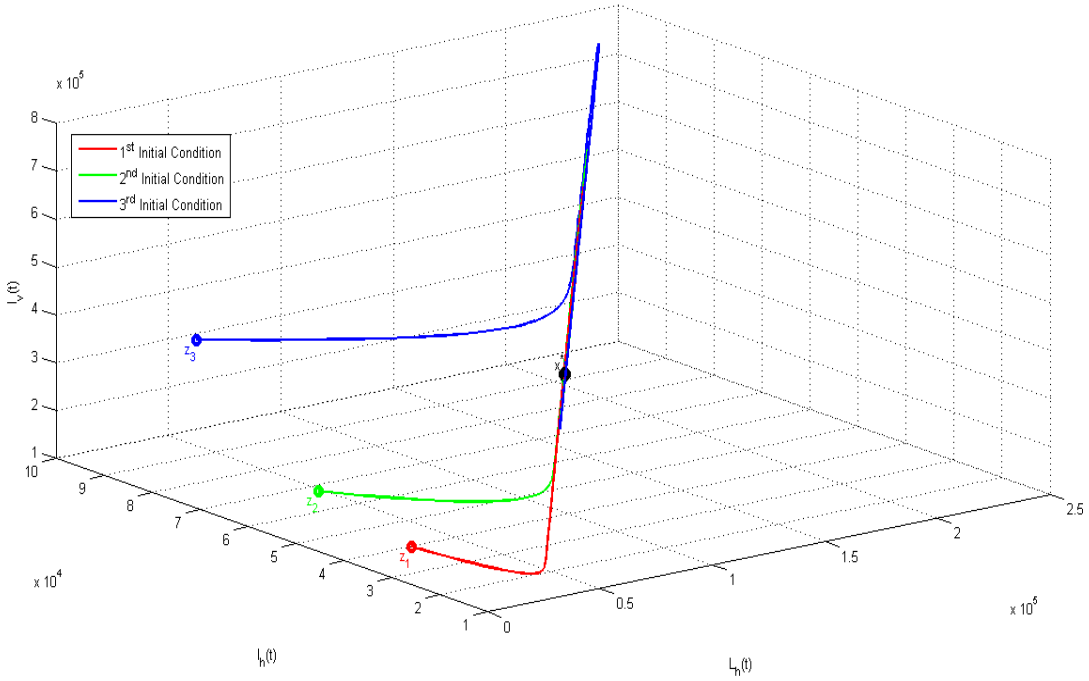

Figure 4. Phase Field of A_h, I_h and I_v Populations

Based on the numerical simulation results shown in **Figure 4**, the trajectories of the A_h, I_h and I_v populations, starting from three different initial conditions, converge to the endemic equilibrium point (x^*), with $R_0 = 1.1326 > 1$. This suggests that the endemic equilibrium point tends to be asymptotically stable when $R_0 > 1$. The foregoing discussion could be summarized in the following theorem.

Theorem 4. *The endemic equilibrium (E^*) of the system tends to be asymptotically stable in the region Ω if $R_0 > 1$.*

3.4 Sensitivity Analysis

This section examines the sensitivity analysis to identify the parameters that significantly influence the basic reproduction number (R_0), as described in **[21]**. Sensitivity analysis allows for the quantification of how changes in parameters affect R_0. The sensitivity index of R_0 with respect to a parameter p is defined as:

$$\Upsilon_p^{R_0} = \frac{\partial R_0}{\partial p} \times \frac{p}{R_0}.$$

Using this formula, sensitivity indices for R_0 were calculated based on the parameter values in **Table 3**. The result is presented in **Table 5**.

Table 5. Sensitivity Index of the Parameters in R_0

Parameters	Sensitivity Index	Parameters	Sensitivity Index
τ	-0.069	β_h	$+0.5$
γ	-0.421	β_v	$+0.5$
Ψ	$+0.166$	μ_h	-0.010
b	$+1$	μ_v	-0.5

A positive sensitivity index means that an increase in the parameter value will cause an increase in the value of R_0. Conversely, a negative sensitivity index means that an increase in the parameter value will cause a decrease in R_0. From **Table 5**, the sensitivity index of the mosquito biting rate (b) is 1, indicate that if the parameter b increase 10%, then the value of R_0 also increase 10%. Conversely, if the parameter b decrease 10%, then the value of R_0 also decrease 10%. Similar proportional relationships hold for other parameters, as shown in **Table 5**. The most influential parameters affecting R_0 are the mosquito biting rate (b), the transmission rate from infected mosquitoes to susceptible humans (β_h), the transmission rate from infected humans to susceptible mosquitoes (β_v), and the mosquito mortality rate (μ_v). This highlights the critical role of vector control strategies in reducing DHF transmission.

3.4.1 Impact Parameters on R_0

The parameter with the highest sensitivity index is b, with an index value of 1. Additionally, the parameters β_h, β_v and μ_v have sensitivity indices of 0.5 and -0.5. These four parameters significantly influence R_0, and their impact has been further analyzed through simulation.

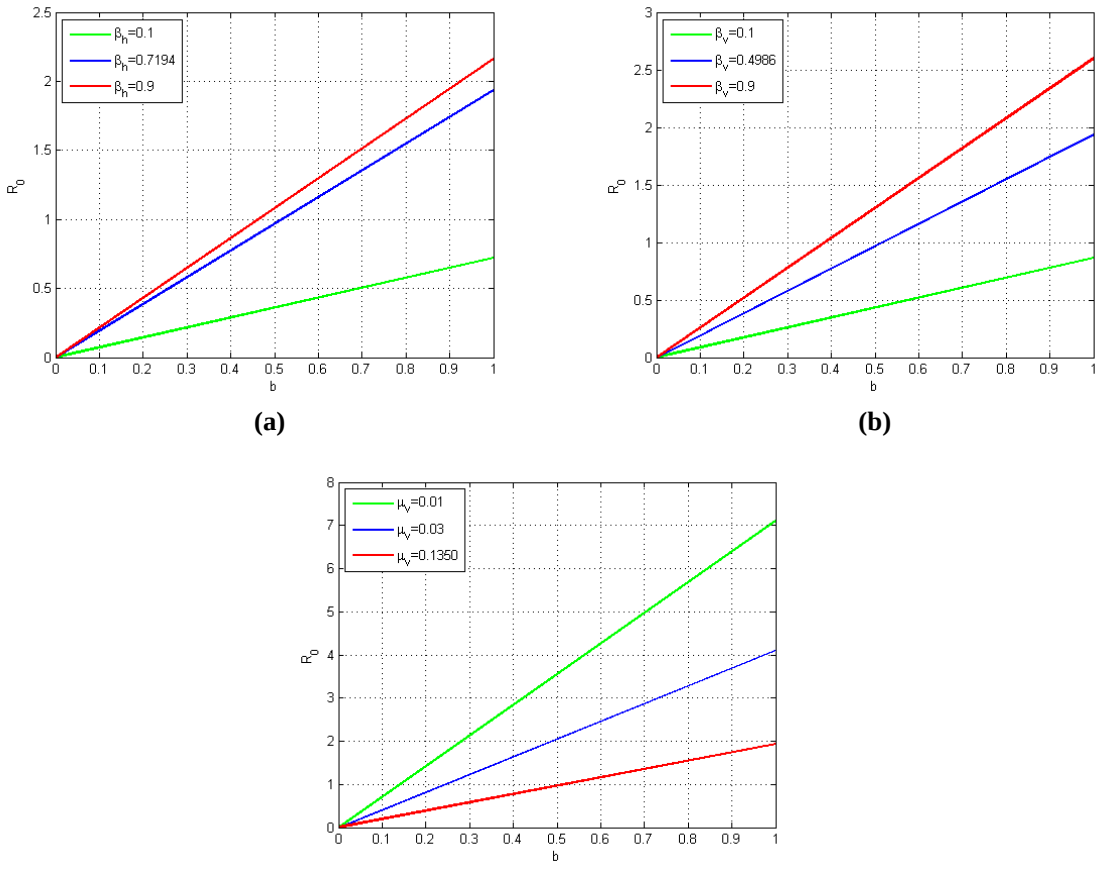

Figure 5. Impact of b on the Value of R_0 with Three Different Values of (a) β_h, (b) β_v and (c) μ_v

Figure 5 illustrates the relationship between these parameters and R_0. It is evident that an increase in b leads to a higher R_0 value, indicating a greater potential for DHF to become endemic. This is because the sensitivity index of b is positive, meaning that an increase in b proportionally increases R_0. Similarly, an increase in β_h and β_v also results in a higher R_0, as both parameters have positive sensitivity indices. In contrast, an increase in μ_v reduces the R_0 value because its sensitivity index is negative. This suggests that higher mosquito mortality can significantly help control the spread of DHF.

3.4.2 Impact Parameters on Population

To further assess the influence of parameters b, β_h, β_v, and μ_v, simulations were conducted to observe their effects on the symptomatic human population (I_h). The resulting simulation graphs are presented in **Figure 6**.

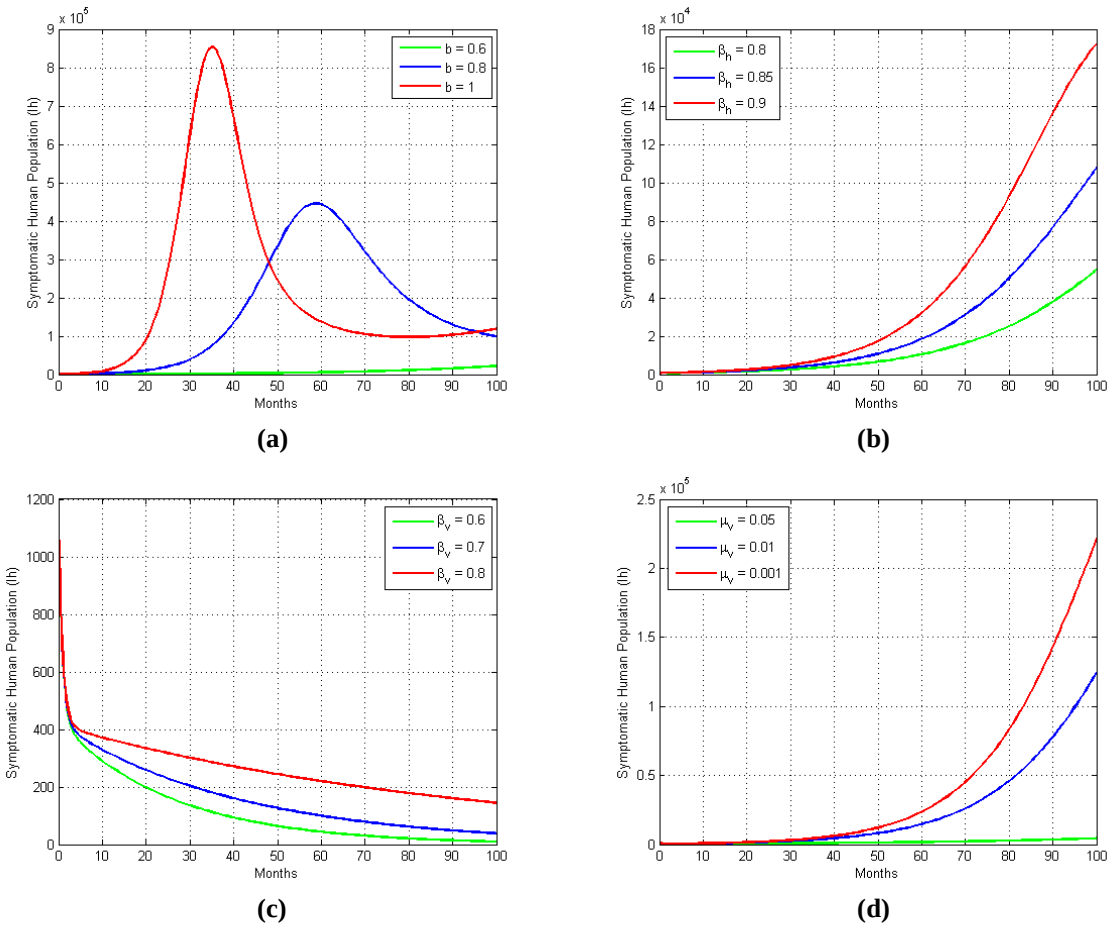

Figure 6. Impact of (a) b, (b) β_h, (c) β_v, and (d) μ_v on I_h

From **Figure 6**, it can be concluded that these four parameters significantly impact changes in the I_h population. When the values of b, β_h, and β_v are low, indicating that a reduced transmission rate leads to the I_h population remains relatively small. Conversely, higher values of these parameters lead to a significant increase in the I_h population, reflecting more intense disease transmission. In contrast, the mosquito mortality rate μ_v exhibits an inverse relationship with the I_h population. When μ_v is high, the transmission rate decreases, resulting in a lower I_h population. However, when μ_v is low, the reduced mosquito mortality allows for more effective disease transmission, leading to an increase in the I_h population.

Since b is the most influential parameter affecting changes in R_0, we further analyze the impact of b on the occurrence of disease-free and endemic conditions. By substituting the parameter values from **Table 3**, except for b, we obtain $R_0 = 1.9351b$. Therefore, for the system to be in a disease-free state when $b < 0.5167700912$, while the system remains endemic when $b > 0.5167700912$.

3.5 Numerical Simulation

To analyze the future trends of dengue hemorrhagic fever (DHF) in West Java, we perform simulations based on the estimated parameter values. The simulations are conducted under two different conditions:

1. Disease-free condition, where parameter values follow **Table 3**, except for $b = 0.3891$, resulting in $R_0 = 0.7529$.
2. Endemic condition, where all parameter values follow **Table 3**, yielding $R_0 = 1.14$.

The numerical simulations are implemented using the Runge-Kutta integration method. The comparison of population dynamics under these two conditions is presented in **Figure 7**. These simulations provide insights into the potential trajectory of DHF in West Java Province.

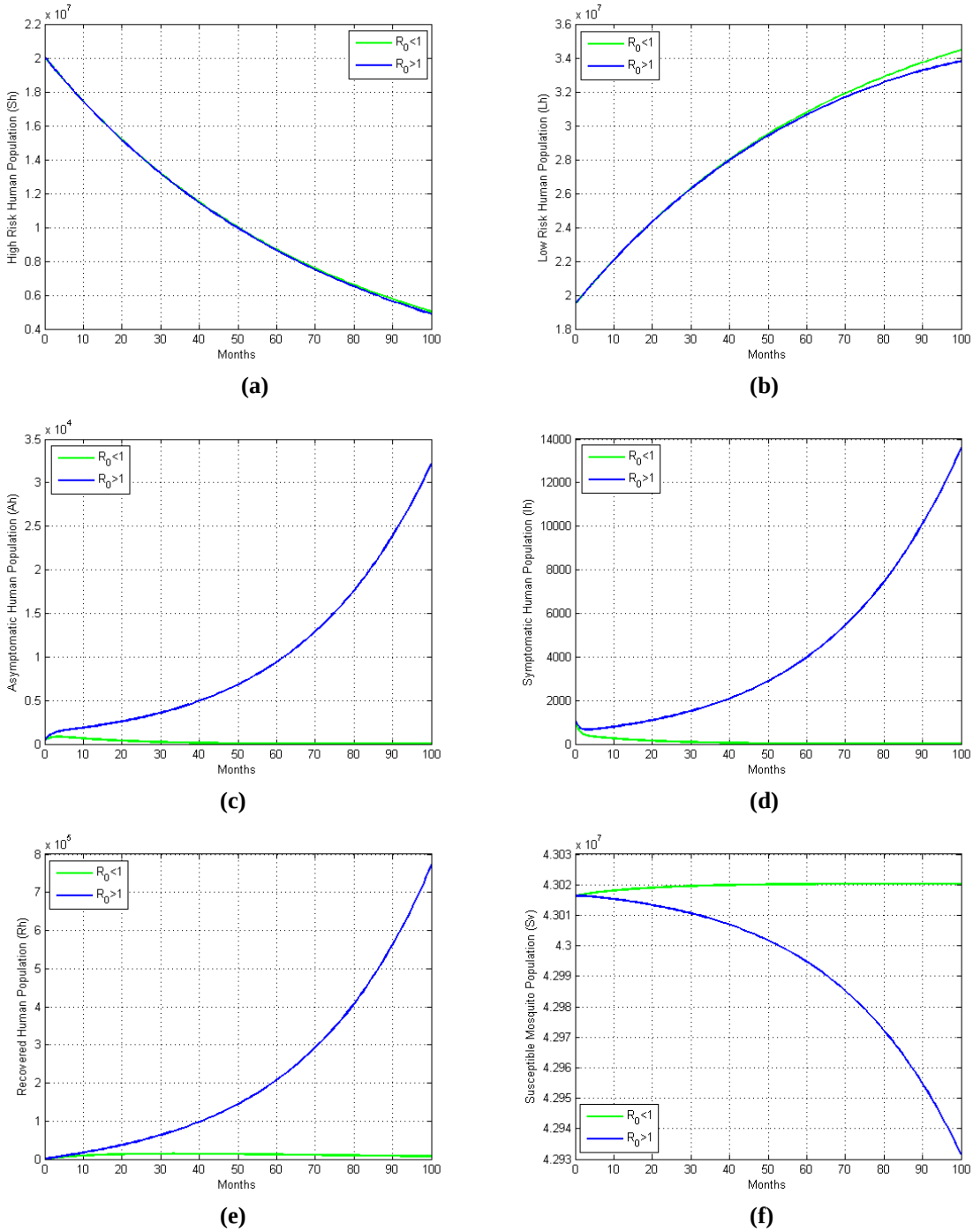

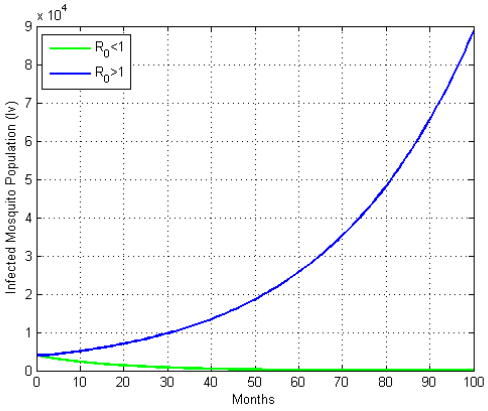

(g)

Figure 7. Numerical simulation of (a) S_h, (b) L_h, (c) A_h, (d) I_h, (e) R_h, (f) S_v, and (g) I_v population

The results indicate that when $R_0 > 1$, the disease persists in the population, leading to an increase in the number of infected individuals over time. In contrast, when $R_0 < 1$, the infection gradually dies out. This condition aligns with our previous calculations, which show that the system remains in a disease-free state when $b < 0.5167700912$, while it stays endemic when $b > 0.5167700912$. Therefore, controlling and reducing the mosquito biting rate (b) can be one of the key strategies for shifting the system toward a disease-free state. These findings underscore the critical threshold behavior of R_0 and emphasize the necessity of maintaining control efforts to prevent periodic resurgences of DHF outbreaks.

4. CONCLUSIONS

This study developed a mathematical model to analyze the transmission dynamics of Dengue Hemorrhagic Fever (DHF) in East Java Province, Indonesia. The model integrates key epidemiological different levels of transmission risk and utilizes a Genetic Algorithm (GA) to optimize parameter estimation. The basic reproduction number (R_0) was calculated as 1.0959, confirming the endemic status of DHF in West Java Province in 2018. Stability analysis demonstrated that the disease-free equilibrium is locally and globally asymptotically stable when $R_0 < 1$, while the endemic equilibrium tends to be asymptotically stable when $R_0 > 1$. Sensitivity analysis revealed that the mosquito biting rate (b), mosquito mortality rate (μ_v), and transmission rates from infected mosquitoes to humans (β_h) and from infected humans to mosquitoes (β_v) are the most critical factors influencing the basic reproduction number (R_0). Among these, parameter b exhibited the highest sensitivity index, indicating a direct proportional relationship. Next, the most influential parameters are β_h and β_v, which have a positive sensitivity index, as well as μ_v, which has a negative sensitivity index. Simulations further analyzed the effects of these four parameters on both R_0 and the symptomatic human population (I_h). The results confirmed that higher values of b, β_h, and β_v increase R_0 and amplify I_h, reflecting intensified transmission dynamics. For instance, a significant rise in b or β_h leads to a marked increase in the peak and duration of I_h, highlighting their impact on disease propagation. In contrast, an increase in μ_v reduces R_0 and diminishes I_h, indicating its crucial role in suppressing outbreaks. These findings underscore the importance of vector control measures targeting b and μ_v, such as fumigation and environmental interventions to eliminate breeding sites. By effectively reducing b and increasing μ_v, public health efforts can achieve significant reductions in both R_0 and I_h.

REFERENCES

[1] World Health Organization, "DENGUE GUIDELINES, FOR DIAGNOSIS, TREATMENT, PREVENTION AND CONTROL." Accessed: Sep. 19, 2020. [Online]. Available: https://www.who.int/publications/i/item/9789241547871

[2] D. J. Gubler, "DENGUE AND DENGUE HEMORRHAGIC FEVER," *Clin. Microbiol. Rev.*, vol. 11, no. 3, pp. 480–496, 1998, https://doi.org/10.1016/B978-0-443-06668-9.50077-6.

[3] A. Wilder-Smith, E. E. Ooi, S. G. Vasudevan, and D. J. Gubler, "UPDATE ON DENGUE: EPIDEMIOLOGY, VIRUS EVOLUTION, ANTIVIRAL DRUGS, AND VACCINE DEVELOPMENT," *Curr. Infect. Dis. Rep.*, vol. 12, no. 3, pp. 157–

164, 2010, https://doi.org/10.1007/s11908-010-0102-7.
[4] World Health Organization, "GLOBAL STRATEGY FOR DENGUE PREVENTION AND CONTROL, 2012–2020." Accessed: Sep. 19, 2020. [Online]. Available: https://www.who.int/publications/i/item/9789241504034
[5] Health Department of East Java Province Indonesia, "PROFIL KESEHATAN PROVINSI JAWA TIMUR TAHUN 2018," DINAS KESEHATAN PROVINSI JAWA TIMUR. Accessed: Sep. 19, 2020. [Online]. Available: https://dinkes.jatimprov.go.id/index.php?r=site/file_list&id_file=10&id_berita=8
[6] Ministry of Health of the Republic Indonesia, "PROFIL KESEHATAN INDONESIA TAHUN 2017." Accessed: Sep. 19, 2020. [Online]. Available: https://www.kemkes.go.id/id/profil-kesehatan-indonesia-2017
[7] E. Bonyah, M. L. Juga, C. W. Chukwu, and Fatmawati, "A FRACTIONAL ORDER DENGUE FEVER MODEL IN THE CONTEXT OF PROTECTED TRAVELERS," *Alexandria Eng. J.*, vol. 61, no. 1, pp. 927–936, 2022, https://doi.org/10.1016/j.aej.2021.04.070.
[8] D. Handayani, A. U. Gunadi, and R. N. Rachmawati, "MATHEMATICAL MODEL OF REPELLENT EFFECT IN DENGUE TRANSMISSION," *BAREKENG J. Math. Its Appl.*, vol. 18, no. 2, pp. 1037–1052, May 2024, https://doi.org/10.30598/barekengvol18iss2pp1037-1052.
[9] T. P. Blante, J. Jaharuddin, and E. H. Nugrahani, "SENSITIVITY ANALYSIS OF SI1I2RS MODEL FOR DENGUE FEVER TRANSMISSION," *Jambura J. Biomath.*, vol. 5, no. 1, pp. 19–26, 2024, https://doi.org/10.37905/jjbm.v5i1.23132.
[10] A. Abidemi, Fatmawati, and O. J. Peter, "AN OPTIMAL CONTROL MODEL FOR DENGUE DYNAMICS WITH ASYMPTOMATIC, ISOLATION, AND VIGILANT COMPARTMENTS," *Decis. Anal. J.*, vol. 10, no. June 2023, p. 100413, 2024, https://doi.org/10.1016/j.dajour.2024.100413.
[11] F. B. Agusto and M. A. Khan, "OPTIMAL CONTROL STRATEGIES FOR DENGUE TRANSMISSION IN PAKISTAN," *Math. Biosci.*, vol. 305, no. July, pp. 102–121, 2018, https://doi.org/10.1016/j.mbs.2018.09.007.
[12] R. Jan, M. A. Khan, P. Kumam, and P. Thounthong, "MODELING THE TRANSMISSION OF DENGUE INFECTION THROUGH FRACTIONAL DERIVATIVES," *Chaos, Solitons and Fractals*, vol. 127, pp. 189–216, 2019, https://doi.org/10.1016/j.chaos.2019.07.002.
[13] I. Ghosh, P. K. Tiwari, and J. Chattopadhyay, "EFFECT OF ACTIVE CASE FINDING ON DENGUE CONTROL: IMPLICATIONS FROM A MATHEMATICAL MODEL," *J. Theor. Biol.*, vol. 464, pp. 50–62, 2019, https://doi.org/10.1016/j.jtbi.2018.12.027.
[14] N. Anggriani, H. Tasman, M. Z. Ndii, A. K. Supriatna, E. Soewono, and E. Siregar, "THE EFFECT OF REINFECTION WITH THE SAME SEROTYPE ON DENGUE TRANSMISSION DYNAMICS," *Appl. Math. Comput.*, vol. 349, pp. 62–80, 2019, https://doi.org/10.1016/j.amc.2018.12.022.
[15] H. Zhang and R. Lui, "RELEASING WOLBACHIA-INFECTED AEDES AEGYPTI TO PREVENT THE SPREAD OF DENGUE VIRUS: A MATHEMATICAL STUDY," *Infect. Dis. Model.*, vol. 5, pp. 142–160, 2020, https://doi.org/10.1016/j.idm.2019.12.004.
[16] N. Aldawoodi, "AN APPROACH TO DESIGNING AN UNMANNED HELICOPTER AUTOPILOT USING GENETIC ALGORITHMS AND SIMULATED ANNEALING," University of South Florida, 2008. [Online]. Available: https://www.proquest.com/openview/416ccc976083ba5055b263f0787304e9/1?pq-origsite=gscholar&cbl=18750
[17] Central Bureau of Statistics East Java Province Indonesia, "ANGKA HARAPAN HIDUP (TAHUN), 2017-2019." Accessed: Sep. 19, 2020. [Online]. Available: https://jatim.bps.go.id/id/statistics-table/2/MjkjMg==/angka-harapan-hidup.html
[18] Central Bureau of Statistics East Java Province Indonesia, "JUMLAH PENDUDUK MENURUT JENIS KELAMIN DAN KABUPATEN/KOTA PROVINSI JAWA TIMUR (JIWA), 2016-2018." [Online]. Available: https://jatim.bps.go.id/id/statistics-table/2/Mzc1IzI=/jumlah-penduduk-menurut-jenis-kelamin-dan-kabupaten-kota-provinsi-jawa-timur.html
[19] P. Van Den Driessche and J. Watmough, "REPRODUCTION NUMBERS AND SUB-THRESHOLD ENDEMIC EQUILIBRIA FOR COMPARTMENTAL MODELS OF DISEASE TRANSMISSION," *Math. Biosci.*, vol. 180, no. 1–2, pp. 29–48, 2002, https://doi.org/10.1016/S0025-5564(02)00108-6.
[20] J. P. LaSalle, *THE STABILITY OF DYNAMICAL SYSTEMS*. Philadelphia: Society for Industrial and Applied Mathematics, 1976.
[21] N. Chitnis, J. M. Hyman, and J. M. Cushing, "DETERMINING IMPORTANT PARAMETERS IN THE SPREAD OF MALARIA THROUGH THE SENSITIVITY ANALYSIS OF A MATHEMATICAL MODEL," *Bull. Math. Biol.*, vol. 70, no. 5, pp. 1272–1296, 2008, https://doi.org/10.1007/s11538-008-9299-0.